



Gas permeability of needle perforated films

Confidential report for Multivac

Dr. E.U. Thoden van Velzen

Report 615



Gas permeability of needle perforated films

Confidential report for Multivac

Dr. E.U. Thoden van Velzen

Report 615

2250833

Colophon

Title	Gas permeability of needle perforated films
Author(s)	E.U. Thoden van Velzen
AFSG number	615
ISBN-number	none
Date of publication	3 February 2006
Confidentiality	YES
OPD code	06/017
Approved by	Henry Boerriqter

Agrotechnology and Food Sciences Group
P.O. Box 17
NL-6700 AA Wageningen
Tel: +31 (0)317 475 024
E-mail: info.afsg@wur.nl
Internet: www.afsg.wur.nl

© Agrotechnology and Food Sciences Group

Alle rechten voorbehouden. Niets uit deze uitgave mag worden verveelvoudigd, opgeslagen in een geautomatiseerd gegevensbestand of openbaar gemaakt in enige vorm of op enige wijze, hetzij elektronisch, hetzij mechanisch, door fotokopieën, opnamen of enige andere manier, zonder voorafgaande schriftelijke toestemming van de uitgever. De uitgever aanvaardt geen aansprakelijkheid voor eventuele fouten of onvolkomenheden.

All rights reserved. No part of this publication may be reproduced, stored in a retrieval system of any nature, or transmitted, in any form or by any means, electronic, mechanical, photocopying, recording or otherwise, without the prior permission of the publisher. The publisher does not accept any liability for inaccuracies in this report.



The quality management system of Agrotechnology and Food Sciences Group is certified by SGS International Certification Services EESV according to ISO 9001:2000.

Abstract

Multivac has requested A&F to determine the gas permeability coefficients of newly developed needle perforated packages. These permeability values were found to be in the range of 10,000 – 40,000 ml/m².bar.day for oxygen, nitrogen and carbon dioxide, or 20-55 ml/perforation.bar.day. These results were found to possess a major variance. SEM images were taken of the perforations to study the structure of the perforations. Most of the perforations were found to be partially blocked with residual material. Most likely, material that has been displaced by the needle entering the film is pulled inside the perforation when the needle is retracted. It is likely that this can be reduced and possibly be avoided with less flexible, glassier polymeric films such as PP and APET. Therefore, it is recommended to first study the effect of this type of needle perforation with SEM on several polymeric films and to subsequently measure the permeability of well-perforated films.

Content

Abstract	3
1 Introduction	7
2 Methods	9
2.1 Permeability measurements	9
3 Results	11
3.1 Gas permeability values of the perforated packages	11
3.2 Light microscopy	14
3.3 Scanning electron microscopy	14
3.4 Theoretical prediction of the permeability values	16
4 Conclusions	19
Acknowledgements	21
Appendices	23

1 Introduction

Multivac is developing a new line of equilibrium modified atmosphere packages intended for respiring fruits and vegetables. This new packaging concept is based on thermoformed trays with top-lids that have been microperforated in the top-film with a very thin needle. It is the intention that active gas packaging (flushing the content with an ideal gas mixture prior to sealing) will be combined with passive gas packaging (based on the interaction between gas exchange through the perforations and respiration).

In this first project it was intended to determine the gas permeability values of the first concepts. These first two concepts were trays of 22 x 11 x 2 cm made of APET / PE (350 μm) and top-lids made of PET / PE / EVOH / PE (80 μm). The first concept had 21 perforations in the top-film and the second 42 perforations. These will be named “21” and “42” throughout this report.

2 Methods

2.1 Permeability measurements

On four of each packaging concepts syringes were introduced in the side walls of the thermoformed trays and these were glued with a special silicon kit to form a non-leaking gas connection. These packages were flushed with carbon dioxide gas, placed in an acclimatised room at 7°C and subsequently connected to a Chrompack Micro GC CP 2002 gas chromatograph for air gases (O₂, CO₂ and N₂) with 16 channels. These eight packages were sampled nearly every 16 minutes and gas chromatographs were recorded. These rough GC-curves were automatically converted into volume percentages air gases. At the end of experiment (after half a day) a list of times and gas compositions of the internal packaging atmospheres were given and used as input to calculate the permeability values.

Gas permeability values were calculated from the gas composition data from the packaging headspaces from the differentials in gas volumes in times, these were normalised for the partial pressure gradient and the total packaging surface or amount of perforations present.

3 Results

3.1 Gas permeability values of the perforated packages

The development of the gas composition within the packages with 21 perforations is shown in Figure 1. These four graphs are clearly different; packages 21-5 and 21-6 are clearly more permeable than 21-1 and 21-2. The carbon dioxide levels started rather high at levels of 60-80 %. Within the lesser permeable packs the carbon dioxide level decreased from 80 to 50 % in half a day's time. Within the more permeable packs the carbon dioxide level decreased from 60 to 30 % in half a day's time. The gas permeability values calculated from these graphs are summarised in Table 1.

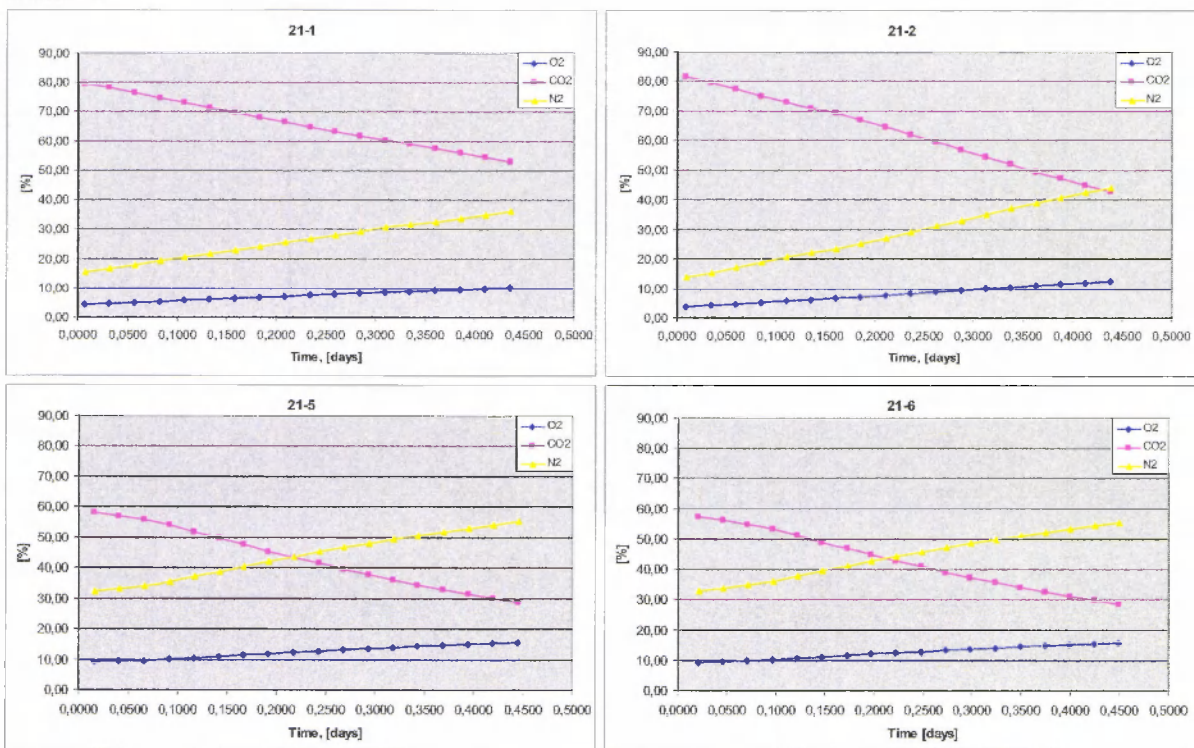


Figure 1: Development of the gas compositions within the headspaces of the four packages with 21 perforations at 7°C.

Table 1: Calculated gas permeability values for packages with 21 perforations at 7°C.

Package	Oxygen		Carbon dioxide		Nitrogen	
	ml/m ² .bar.day	ml/hole.bar.day	ml/m ² .bar.day	ml/hole.bar.day	ml/m ² .bar.day	ml/hole.bar.day
21-1	11900 ± 1000	36 ± 3	10200 ± 300	30 ± 1	10000 ± 400	30 ± 1
21-2	18600 ± 4000	56 ± 11	16000 ± 3400	47 ± 10	15000 ± 3400	46 ± 10
21-5	24500 ± 2000	73 ± 6	19100 ± 400	57 ± 1	18000 ± 300	55 ± 1
21-6	24300 ± 1500	73 ± 5	19000 ± 400	56 ± 1	18000 ± 300	54 ± 1

These calculated permeability values further clarify the large spread in results between individual packages. The oxygen permeability values range from 36 ± 3 to 73 ± 5 ml O₂/hole.bar.day, which is a factor two difference. Such a large deviation in results is unacceptable, makes simple averaging of the results impossible and hints at physical reasons for the large deviation.

The gas development inside the packages with 42 perforations is shown in Figure 2. These graphs show a substantial deviation between each other. Package 42-7 shows the highest permeability and package 42-3, 42-4 and 42-8 are slightly less permeable. The calculated permeability values are summarised in Table 2.

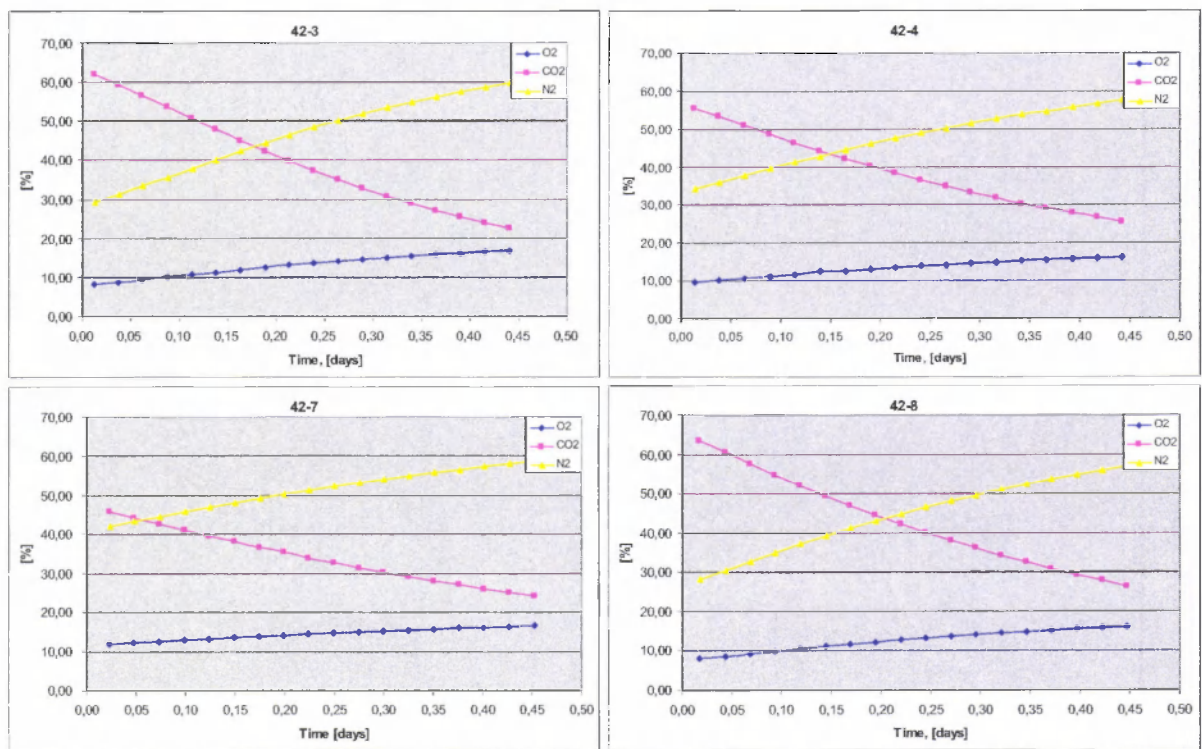


Figure 2: Development of the gas compositions within the headspaces of the four packages with 42 perforations at 7°C.

Table 2: Calculated gas permeability values for packages with 42 perforations at 7°C

Package	Oxygen		Carbon dioxide		Nitrogen	
	ml/m ² .bar.day	ml/hole.bar.day	ml/m ² .bar.day	ml/hole.bar.day	ml/m ² .bar.day	ml/hole.bar.day
42-3	35000 ± 1700	53 ± 3	26300 ± 400	39 ± 1	25300 ± 500	38 ± 1
42-4	27000 ± 1000	40 ± 2	19500 ± 400	29 ± 1	19000 ± 1400	29 ± 2
42-7	22400 ± 1900	33 ± 3	16000 ± 800	24 ± 1	21000 ± 400	31 ± 1
42-8	29000 ± 1700	43 ± 3	22000 ± 300	33 ± 1	15000 ± 900	23 ± 1

Both group of perforated packages with either 21 or 42 perforations possess permeability values that are clearly in the range of microperforated films (7,000 – 100,000 ml/m².day.bar), but possess a too large standard deviation to allow practical use. This large deviation is likely to stem not from the measurement itself but some type of technical variation in the packaging production process.

A second permeability test was performed with partially the same and partially other packages to exclude methodical errors due to the very high initial CO₂ levels of the first test. This time the initial atmosphere was not 80 % CO₂ but in stead 30 % CO₂, 30 % O₂ and 40 % N₂. The results are summarised in Table 3 and Table 4. The graphs are shown in the appendix. The spread in results is little bit less but still large.

An improvement can still be observed in the permeability levels per hole. These levels are now in same range for both the packages with 21 and 42 perforations, making these values more reliable than those from the first permeability test. For oxygen this value is about 38 ±10, for carbon dioxide 35 ±10 and 37 ± 10 for nitrogen ml/hole.day.bar.

Table 3: Calculated gas permeability values for packages with 21 perforations at 7°C, resulting from the second measurement test.

Package	Oxygen		Carbon dioxide		Nitrogen	
	ml/m ² .bar.day	ml/hole.bar.day	ml/m ² .bar.day	ml/hole.bar.day	ml/m ² .bar.day	ml/hole.bar.day
21-1	10300 ± 300	31 ± 1	9200 ± 300	27 ± 1	9700 ± 300	30 ± 1
21-2	17000 ± 2000	49 ± 7	15000 ± 4000	44 ± 11	16000 ± 3400	47 ± 10
21-6	18000 ± 3000	54 ± 8	17000 ± 3000	50 ± 10	18000 ± 3000	52 ± 10
21-9	13800 ± 600	41 ± 2	12900 ± 800	38 ± 3	13600 ± 700	41 ± 2
21-10	12700 ± 500	38 ± 2	13000 ± 1000	37 ± 3	13200 ± 900	39 ± 3

Table 4: Calculated gas permeability values for packages with 42 perforations at 7°C, resulting from the second measurement test.

Package	Oxygen		Carbon dioxide		Nitrogen	
	ml/m ² .bar.day	ml/hole.bar.day	ml/m ² .bar.day	ml/hole.bar.day	ml/m ² .bar.day	ml/hole.bar.day
42-3	23000 ± 1600	35 ± 2	24000 ± 800	36 ± 1	25000 ± 800	37 ± 1
42-4	17000 ± 800	25 ± 1	18200 ± 300	27 ± 1	18900 ± 300	28 ± 1
42-7	14100 ± 700	21 ± 1	15100 ± 400	22 ± 1	15500 ± 400	23 ± 1
42-11	32000 ± 5000	47 ± 7	37500 ± 400	56 ± 1	38000 ± 1100	57 ± 2
42-12	18600 ± 800	28 ± 1	18400 ± 400	28 ± 1	19300 ± 300	29 ± 1

3.2 Light microscopy

In order to understand the reason for this large deviation better and to enable a theoretical prediction of the expected permeability values based on the diameter of the perforations the perforations were studied with light microscopy and scanning electron microscopy.

Samples were cut from the perforated top-film and clamped on microscope glasses and enlarged for 400x times to allow visual inspection. The perforations could clearly be observed. The internal diameter of the perforation was on average $93 \pm 10 \mu\text{m}$ (8 perforations averaged), the external diameter was $137 \pm 20 \mu\text{m}$. On most perforations small side cuts were observed, which extended about $50 \mu\text{m}$ outwards from the perforation see Figure 3. In general the internal perforation diameter was reasonably round. At focus depths corresponding to heights below the surface of the film the perforations appeared to narrow. However, it was very difficult to get clear images from inside the perforations.

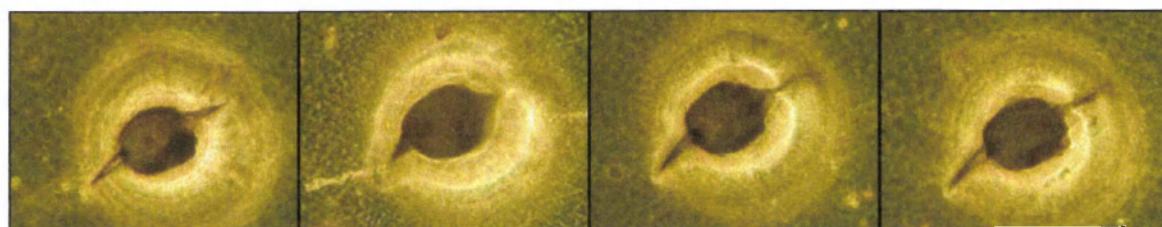


Figure 3: Four light microscopy pictures at 400x enlargement of four different perforations observed from the upside of the film and focussed on the film surface.

3.3 Scanning electron microscopy

Scanning electron microscopy (SEM) pictures of the perforations were made to study the size and internal structure of the perforations better. Therefore samples of the perforated film were sputter-coated with gold in vacuum and studied at various magnification levels. Figure 4 shows two typical overview SEM images of the perforations, one from the upside and one from the downside of the film. A major asymmetry is directly noticed in the perforation structure.

The upside (outside surface of the top-film) has a cupola of $200 \mu\text{m}$ large with a large straight crevice splitting it in two halves and with more or less material in the centre of the crevice.

The downside of the perforation is a clear crater-type hole, with indeed an internal diameter of about $90 \mu\text{m}$ and an outer diameter of about $150 \mu\text{m}$.

This observed asymmetry confirms the direction at which the needle has exited the film. First it was punched from the upside through the film and subsequently it was retracted from below to above, creating a crater on the downside and a cupola on the upside. The material that should have been removed by the needle to form the perforation appears to have been pulled into the perforation by the exiting needle.

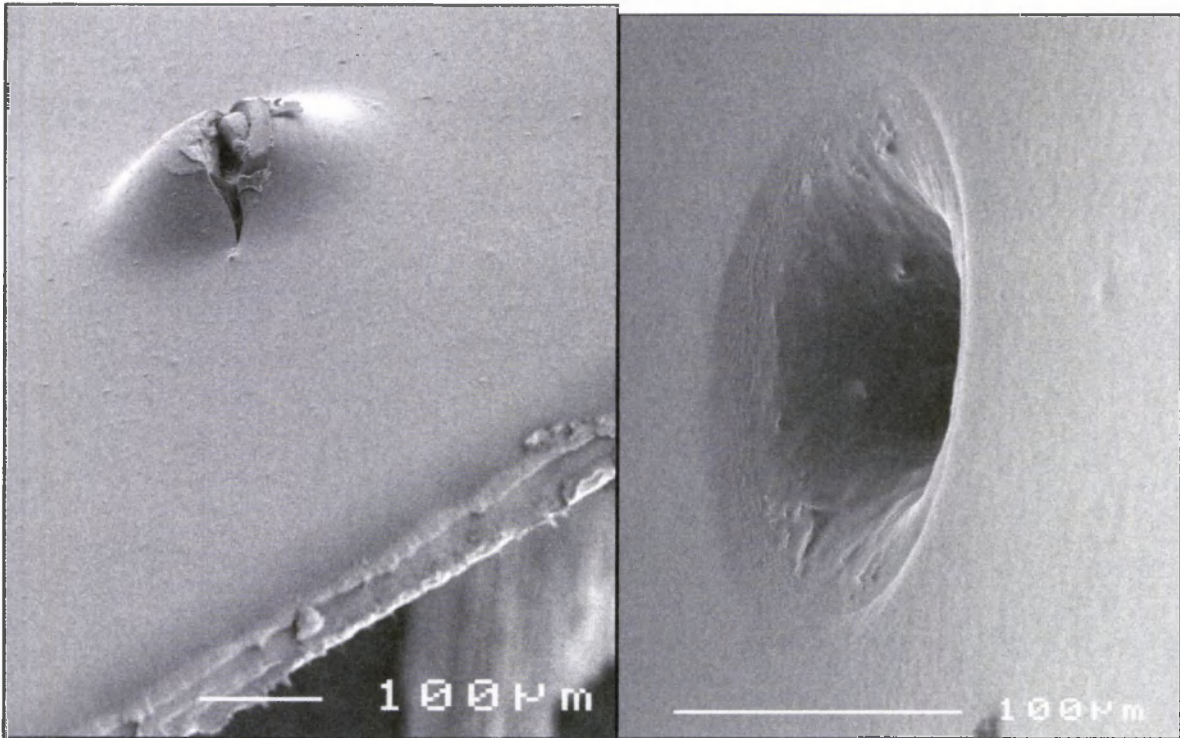


Figure 4: Overview SEM images from the upside of the perforated film (left) and from the downside of the perforated film (right). Enlargement factor 100x.

In order to get a good impression of the perforation-structure several detail SEM images were made perpendicular to the film directly over the perforation with an enlargement factor of 1000, see Figure 5.

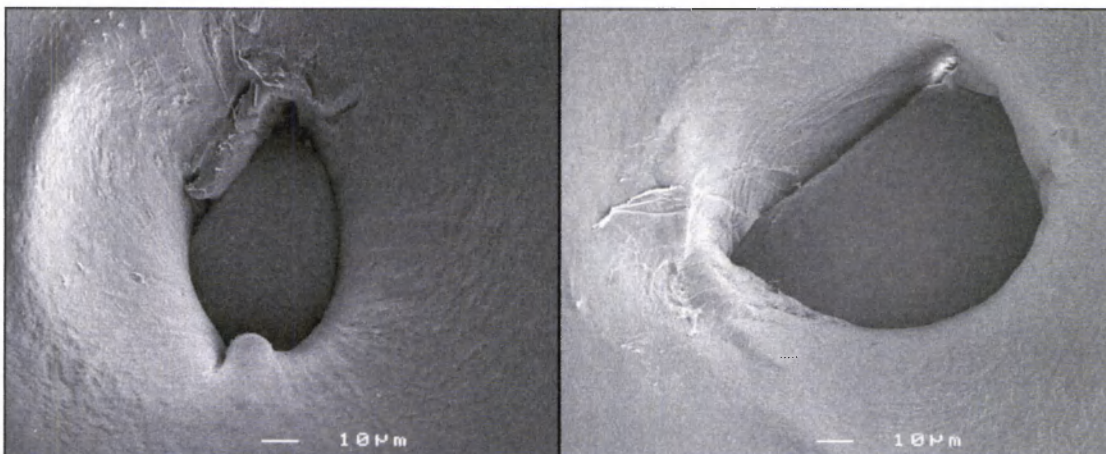


Figure 5: SEM images from the downside of the film showing the inside of two different perforations made with an enlargement factor of 1000x.

Surprisingly, the perforations appeared to be (partially) filled with residual material. The material that has to be removed by the needle to form perforations has apparently not been removed completely. Probably this residual material has not been cut loose from the film completely and has been pulled back into the perforation by the exiting needle.

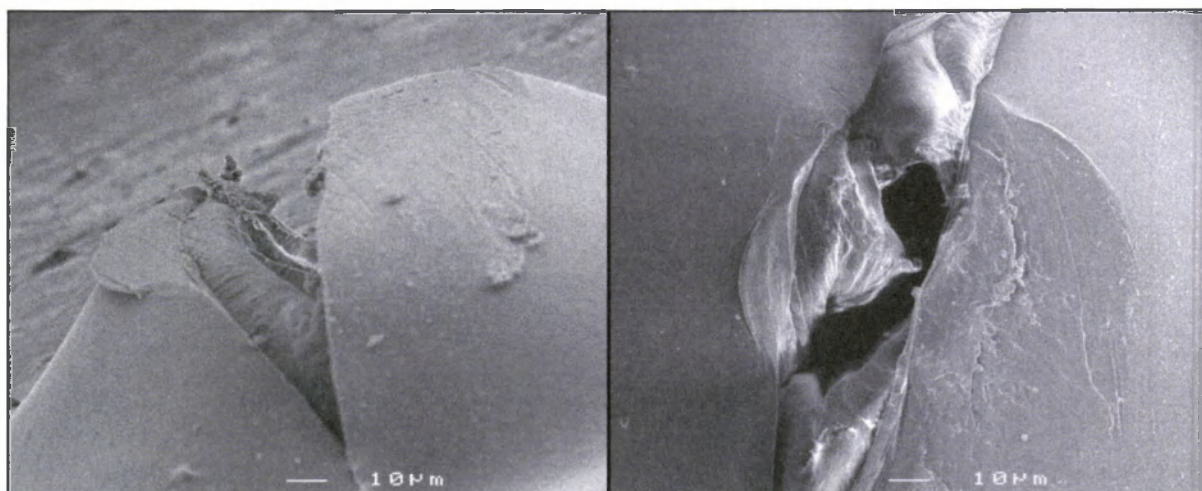


Figure 6: SEM images from the upside of the film showing two different perforations in more detail from two different angles, 1000x enlarged.

Figure 6 clearly shows that the four different polymer layers of the top-film are partially delaminated near the perforation. Some of these layers show a larger tendency to fill the perforation than others, more precisely the PET-layer (top in figure 6) does not appear to fold back into the hole, whereas the PE / EVOH layers do appear to fill the hole.

3.4 Theoretical prediction of the permeability values

Based on the measured perforation sizes of 90 μm , the theoretical permeability values were calculated with the Knudsen diffusion flux equation, see Equation 1. The obtained predictions for the packages with 21 perforations are summarised in Table 5.

Table 5: Gas permeability values calculated with the Knudsen diffusion equation.

Gas	Gas gradient		Total permeability [ml/m ² .bar.day]	
	Outside [%]	Inside [%]	21 holes	42 holes
Oxygen	20	30	870,000	1,700,000
Carbon dioxide	0.05	20	2,950,000	5,900,000
Nitrogen	79	50	7,800,000	15,600,000

This theoretical permeability prediction shows that when the packages possessed 21 or 42 perfect round perforations that the permeability values would be much higher than what was actually measured. The difference is about a factor 70 for oxygen, about a factor 200 for carbon dioxide and about a factor 600 for nitrogen. This proves that the perforations are not open cylinders and that a more complicated diffusion mechanism prevails over Knudsen diffusion (otherwise the same difference factors would have been observed for all gases). This hints that many gas molecules will actually diffuse through pores of about 0.1 μm diameter and less.

$$J_k = \frac{2.r\varepsilon}{3.X} \sqrt{\frac{8RT}{\pi M}} \left\{ \frac{M.\Delta P}{RT.\delta} \right\}$$

- J_k : Flux [$\text{kg}/\text{m}^2.\text{s}$]
- r : Pore diameter: 90 μm
- ε : Porosity: number of perforations per $\text{m}^2 * (\pi/4) * r^2$ [m^2/m^2]
- X : Tortuosity: 1 m/m
- T : Temperature: 7°C
- M : molecular weight permeant g/mole
- ΔP : pressure gradient over the film [Pa]
- δ : film thickness: 80 μm

Equation 1: Knudsen diffusion flux equation

If we apply the Knudsen diffusion equation in the reversed manner and enter the measured permeability values and calculate what diameter pores correspond to that, we obtain the following results for the packages with 21 perforations: for oxygen the pore diameter is 23 μm , for nitrogen 11 μm and for carbon dioxide 15 μm . This reconfirms that the actual perforations are much smaller than the 90 μm seen with light microscopy and supports the conclusion of the SEM images that suggest that the pores are partially blocked.

4 Conclusions

Needle perforating the top-films of the Multivac packages enhances the gas permeability of these packages. The resulting permeability values are in the order of 10,000 – 40,000 ml/ m².day.bar which is indeed in the range of microperforated films. However, the variance in the measured gas permeability values is very large. This large standard deviation in permeability stems from the perforation technology which appears to result in perforations that are partially filled with material that should have been removed by the needle. This can clearly be observed with SEM. This partial filling is not reproducible and causes the large variance in permeability results.

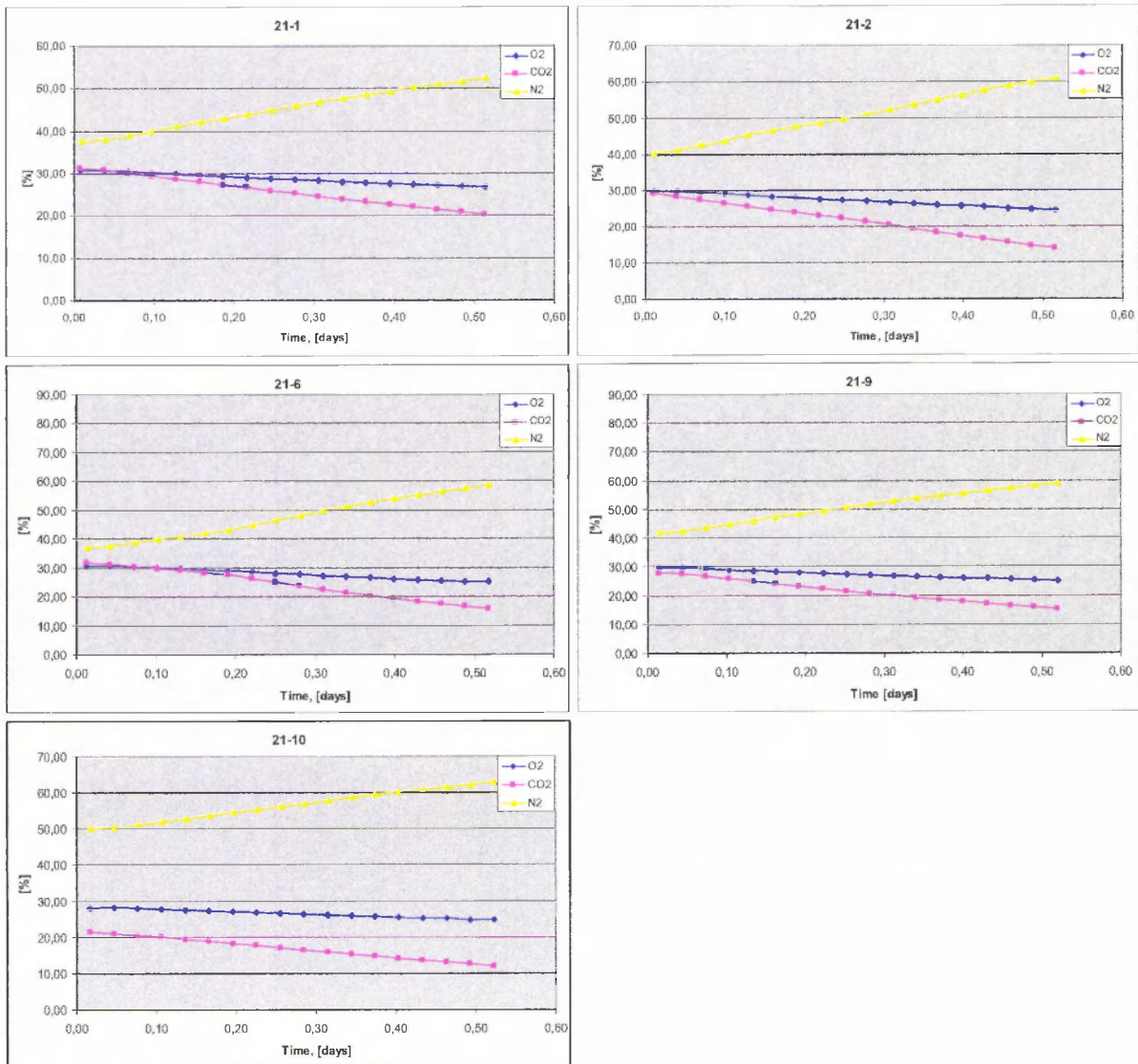
In order to achieve more reproducible open perforations it is necessary to understand the relationship better between polymer film and perforation structures formed by needles in it. In this test a relatively complex top film composed of PET / PE / EVOH / PE was used, which was available on the machines of Multivac to make the perforations. For the future it is wise to test a few mono-materials like PP and APET on perforation structures formed with the needles of Multivac. These structures can best be studied first by SEM and if they are favourable subsequently test the permeability values of the packages with these perforated films.

Acknowledgements

Thanks to Aart Zegveld the gas permeability measurements were performed in a fast and reliable manner. Hetty van der Wal is thanked for helping out with the light microscopes. Jacqueline Donkers is thanked for making the SEM images at the Wageningen University.

Appendices

Development of gas composition in the headspace of the packages with 21 perforations in second round of measurements:



Development of gas composition in the headspace of the packages with 42 perforations in second round of measurements:

